Clinical Trials

# Morphometric Analysis of Optic Nerves and Retina from an End-Stage Retinitis Pigmentosa Patient with an Implanted Active Epiretinal Array

*Jeffrey G. Eng,*[1] *Rajat N. Agrawal,*[1,2] *Kevin R. Tozer,*[1] *Fred N. Ross-Cisneros,*[1] *Gislin Dagnelie,*[3] *Robert J. Greenberg,*[4] *Gerald J. Chader,*[1] *James D. Weiland,*[1,2] *Narsing A. Rao,*[1,2] *Alfredo A. Sadun,*[1,2] *and Mark S. Humayun*[1,2]

**Purpose.** To characterize optic nerve and retinal changes in a patient with end-stage retinitis pigmentosa (RP) with an implanted active epiretinal array.

**Methods.** A 74-year-old man with end-stage X-linked RP underwent implantation of an epiretinal array over the macula in the right eye and subsequent stimulation until his death at 5 years and 3 months after implantation. The optic nerves from this study patient, as well as those from two age-matched normal patients and two age-matched RP patients, were morphometrically analyzed against two different sets of criteria and compared. The retina underlying the array in the study patient was also morphometrically analyzed and compared with corresponding regions of the retina in the age-matched RP patients.

**Results.** Optic nerve total axon counts were significantly lower in the study patient and RP patients than in normal patients. However, there was no significant difference when comparing total axon counts from the optic nerve corresponding to the patient's implanted right eye versus the optic nerves from the RP patients ($P = 0.59$ and $P = 0.61$ using the two different criteria). Degenerated axon data quantified damage and did not show increased damage in the optic nerve quadrant that retinotopically corresponded to the site of epiretinal array implantation and stimulation. Except for the tack site, there was no significant difference when comparing the retina underlying the array and the corresponding perimacular regions of two RP patients.

**Conclusions.** Long-term implantation and electrical stimulation with an epiretinal array did not result in damage that could be appreciated in a morphometric analysis of the optic nerve and retina. (ClinicalTrials.gov number, NCT00279500.) (*Invest Ophthalmol Vis Sci.* 2011;52:4610–4616) DOI:10.1167/iovs.09-4936

From the [1]Doheny Eye Institute, Los Angeles, California; the [2]Department of Ophthalmology, University of Southern California, Los Angeles, California; the [3]Lions Vision Center, Johns Hopkins University, Baltimore, Maryland; and [4]Second Sight Medical Products, Sylmar, California.

Supported by National Institutes of Health Grant EY03040, Research to Prevent Blindness, and Second Sight Medical Products.

Submitted for publication November 16, 2009; revised June 4, October 20, and November 30, 2010; accepted December 26, 2010.

Disclosure: **J.G. Eng**, None; **R.N. Agrawal**, Second Sight Medical Products (F, C), P; **K.R. Tozer**, None; **F.N. Ross-Cisneros**, None; **G. Dagnelie**, None; **R.J. Greenberg**, Second Sight Medical Products (E), P; **G.J. Chader**, None; **J.D. Weiland**, None; **N.A. Rao**, None; **A.A. Sadun**, None; **M.S. Humayun**, Second Sight Medical Products (F, I, C), P

Corresponding author: Rajat N. Agrawal, Doheny Eye Institute, 1355 San Pablo Street, DVRC 124, Los Angeles, CA 90033; rajagramd@gmail.com.

Microelectronic retinal implants have shown great promise in restoring useful vision in patients with outer retinal degenerative diseases such as retinitis pigmentosa (RP) and age-related macular degeneration.[1–3] Our research group and several others have been investigating epiretinal arrays[4–8] that electrically stimulate the remaining inner retinal neurons. These arrays generate multiple spots of light described as phosphenes, which when viewed in a specific pattern, allow patients to regain some visual function.[9,10]

Six patients have undergone monocular implantation with an epiretinal array (Argus I; Second Sight Medical Products, Sylmar, CA) of 5.5 × 6-mm silicone-platinum electrodes connected to an implanted neural stimulator. We present data from the first patient in this group of six, who had the 16-electrode epiretinal array implanted and has since died. This patient had shown an ability to use the epiretinal prosthesis for simple visual tasks.[11] In the present study, we morphometrically analyzed the patient's optic nerves and retina. This study represents the very first opportunity to histologically characterize changes in a patient with an epiretinal prosthesis implanted with subsequent electrical stimulation. Comparison with appropriate controls yielded valuable information regarding the effects of end-stage RP and long-term epiretinal array implantation and stimulation on both the optic nerve and retina. We anticipated that the retina would show the direct effects of RP and long-term implantation and stimulation, whereas the optic nerve, representing the final common pathway for information processing, would demonstrate more global and indirect effects.

## Materials and Methods

### Study Patient Characteristics

The study patient, at death, was a 79-year-old Caucasian man with an ocular history of X-linked RP, extracapsular cataract extraction with intraocular lens implant in 1983, and rectus surgery in 1970. He had a twin brother with RP, whose medical history consisted of hypertension, hypercholesterolemia, and coronary artery disease.

The subject provided informed consent to participate in a U.S. Food and Drug Administration–approved Investigational Device Exemption study with approval from the Institutional Review Board of the University of Southern California. The research complied with the Declaration of Helsinki.

The patient had undergone three acute stimulations in the right eye: in 1992, 1993, and 1996.[1,12] In 2002, an epiretinal array consisting of 16 platinum electrodes (520 $\mu$m diameter) within a silicone substrate was implanted in the right eye. He had been unable to read print or distinguish colors for the prior 6 years. His visual acuity (VA) in 1992, just before the first acute stimulation, was light perception (LP) in the right eye and hand

motion in the left eye. At the time of implantation, VA was no light perception (NLP) in the right eye and LP in the left eye.

The surgical implantation, electrical stimulation parameters, and array characteristics have been described earlier.[9] Six months after implantation, the patient developed persistent shallow subretinal fluid located superotemporally away from the array site. A vitrectomy and silicone oil infusion was performed without complication. There were never any signs of inflammation or infection. Intraocular pressure remained well controlled.

The array remained fixed over the macula until the patient's death approximately 5 years and 3 months after array implantation, when he suffered a massive brain hemorrhage secondary to an accidental fall. The patient was embalmed 22 hours after being taken off life support, and the eyes were enucleated and fixed in formalin 48 hours after embalming.

## Control Patient Characteristics

RP patient 1 was an 85-year-old Caucasian man with an ocular history of RP and bilateral cataract surgery with intraocular lens placement. His medical history included chronic renal insufficiency and gout. He had a family history of RP, with his father and several first cousins affected. The eyes were enucleated and fixed in 4% paraformaldehyde 18 hours and 39 hours after death, respectively.

RP patient 2 was an 85-year-old Caucasian man with an ocular history of autosomal dominant RP. He had no other medical history, but had a family history of RP with three of five brothers affected. Cause of death was intracranial aneurysm. The eyes were enucleated and fixed in 10% formalin 12 hours after death.

Normal patient 1 was a 74-year-old Caucasian man with an ocular history of cataract surgery with no significant co-morbidities. The cause of death was brain death during elective aneurysm coiling. The eyes were enucleated and fixed in 10% formalin approximately 2 hours and 7 hours after death, respectively. Normal patient 2 was a 75-year-old Caucasian woman with no ocular history. Her medical history included aortic valve replacement, chronic obstructive pulmonary disease, diabetes mellitus, hypertension, and bilateral hip fractures. Cause of death was congestive heart failure and coronary artery disease. The eyes were enucleated and fixed in 10% formalin 11 hours postmortem.

## Tissue Processing for Light Microscopy

Retrobulbar optic nerves were dissected into cross-sectional profiles within 1 mm proximal to the globe to minimize distortion of the retinotopic order of myelinated fibers from retinal ganglion cells that would increase in cross sections of these nerves progressing more posteriorly from the globe.[13] Cross sections were postfixed in half-strength Karnovsky solution (Electron Microscopy Sciences, Hatfield, PA). Lipids associated with myelinated axons (fibers) were preserved with a 2% solution of osmium tetroxide. The tissues were further processed for embedding in resin (PELCO Eponate 12; Ted Pella. Inc., Redding, CA). Semithin sections were cut from these plastic tissue blocks (Diamond Histo Knife; Delaware Diamond Knives, Inc., Wilmington, DE) at 1 $\mu$m on an ultramicrotome (MT-2B; Sorvall, Inc., Newtown, CT). For analysis of the retina, the formalin-fixed globes were dissected horizontally through the entire eye bisecting the optic nerve head and macular region where the array was implanted. The retinas were processed, embedded in paraffin, and serially sectioned at 5 $\mu$m on a retractable microtome.

## Tissue Staining

***Para*-phenylenediamine.** Semithin plastic sections of cross-sectional profiles of optic nerves were stained with *p*-phenylenediamine (PPD) to highlight the myelin around axons[14] from retinal ganglion cells. The chelation of osmium to PPD facilitated the identification of circular profiles of the myelin sheath associated with the majority of axons in the cross sections of retrobulbar optic nerve samples.

**Hematoxylin and Eosin.** Hematoxylin and eosin staining was performed on retinal sections at 100-$\mu$m intervals for general morphology, to aid in delineating landmarks such as the optic nerve head and macula (implantation site of array) for immunohistochemical staining of selected slides.

**Immunohistochemistry: Immunoperoxidase Labeling.** Neurons of the retina were identified by using an indirect method for immunoperoxidase staining with a monoclonal rabbit anti-human neuron-specific enolase (NSE) primary antibody (Dako North America, Inc., Carpinteria, CA) at a 1 to 15,000 dilution. Astrocytes of the retina were identified with a similar immunostaining methodology as with NSE by using a polyclonal rabbit anti-human glial fibrillary acidic protein (GFAP) primary antibody (Dako North America, Inc.) at a 1 to 10,000 dilution. Negative control sections were incubated in antibody diluent (Dako North America, Inc.) in the absence of the primary antibody. All sections for both immunostains (using NSE and GFAP) were then exposed to a goat anti-rabbit secondary antibody conjugated to horseradish peroxidase (HRP) (Dako North America, Inc.). The substrate used to react with the HRP to form a resulting brown reaction product (chromogen) was 3,3′-diaminobenzidine (DAB; Dako North America, Inc.). The retinas were counterstained with Mayer's hematoxylin (Dako North America, Inc.) for nuclear staining, to aid in the identification of cellular and tissue landmarks. The retinas were next dehydrated through graded alcohols, cleared in xylene, and coverslipped with a permanent mounting medium. The stained tissue sections were observed on a light microscope (Axioskop; Carl Zeiss Meditec, Inc., Thornwood, NY). Images were captured by digital camera (Spot II; Diagnostic Instruments, Sterling Heights, MI) and saved to a computer.

## Morphometric Analysis of Optic Nerves

Mean axon densities within each optic nerve quadrant were obtained using light microscope images initially captured by the digital camera (Spot II; Diagnostic Instruments) apically mounted on a standard microscope (Carl Zeiss Meditec, Inc.). The acquired images were obtained at a magnification of 1000× with a 100× oil-immersion objective and were refined for axon counting. The counts were performed in a masked manner and manually to reduce the number of missed axons. However, to help account for the subjective nature of counting axons, two sets of data were collected by using two different counting techniques. Inclusion in the first data set required an axon diameter of greater than 1 $\mu$m, whereas the second data set included axons of all diameters where a space could still be distinguished inside the myelin ring. The criteria corresponding to the first and second data sets will hereafter be referred to as criterion 1 and criterion 2, respectively. To assure equal and accurate sampling, locations for each photo site were calculated in advance. The locations were based on the diameter of the optic nerve and allowed for an equal number of photos placed in all four quadrants as well as an equal number in the inner and outer portions of each of the optic nerves. Thirty-two images for each optic nerve were analyzed to compute mean axon densities and total axon counts. The total axon count for a particular optic nerve was derived from the overall average axon density and the measured optic nerve cross-sectional area. Independent-samples *t*-tests were performed to determine any statistically significant differences in mean axon densities among optic nerve quadrants and among the total axon counts for each optic nerve.

The number of degenerated axon profiles within each quadrant of an optic nerve was determined by completely and methodically scanning each quadrant under a standard light microscope at a magnification of 1000×. All degenerated axon profiles were tallied under blinded conditions, with care taken to avoid missing profiles or counting a profile twice. Criterion 1 defined degenerated axon profiles as darkened profiles for which the myelin ring cannot be distinguished due to staining of the entire structure. Criterion 2 also included macrophages that stained positive for myelin because this signified an axon that had been phagocytosed (Fig. 1). The optic nerve quadrants were designated as temporal, inferior, nasal, and superior based on the landmarks established before separation of the optic nerve from the globe. Degenerated axon profiles were tallied in this manner for all optic nerves.

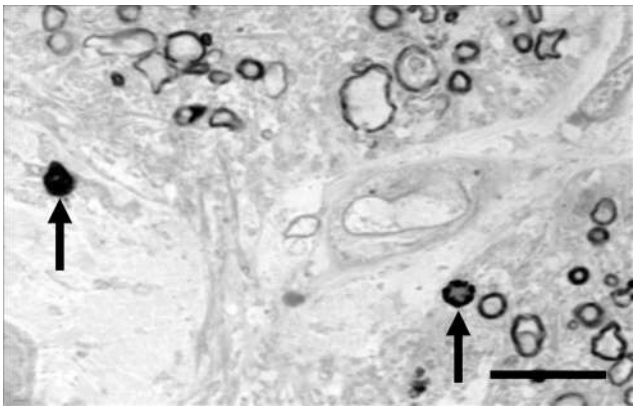

**FIGURE 1.** Degenerated axon profiles. The *arrow* on the *left* indicates an example of a degenerated axon profile that would be counted using criterion 1. A degenerated axon profile represents a late stage of axonal degeneration, during which debris from five to eight individual degenerated axons is surrounded by an intact myelin ring. The *arrow* on the *right* indicates a macrophage that has phagocytosed an axon and thus, stains positive for myelin. Criterion 2 includes both the degenerated axon profiles and macrophages in the degeneration counts. Bar, 10 $\mu$m.

## Morphometric Analysis of the Retina

There was emphasis on analysis of the macula and the perimacular region, since the epiretinal array was implanted directly above that area. The retina underneath the array, or comparable region of the retina in the RP control eyes, was divided into nine equivalent regions in a 3-by-3 grid arrangement (Fig. 2) for analysis. The neurons were sampled in each of the nine regions in the macular and perimacular region. Each region had at least three cross sections in which the neurons were counted.

## RESULTS

A 74-year-old man with X-linked end-stage RP and VA of NLP in the right eye, underwent surgical implantation of a 16-electrode epiretinal prosthesis in that eye. The procedure was followed by electrical stimulation over a period of 5 years and 3 months, during which the patient was able to perceive phosphenes and perform simple tasks using the implanted prosthesis. VA without electronic assistance remained at NLP

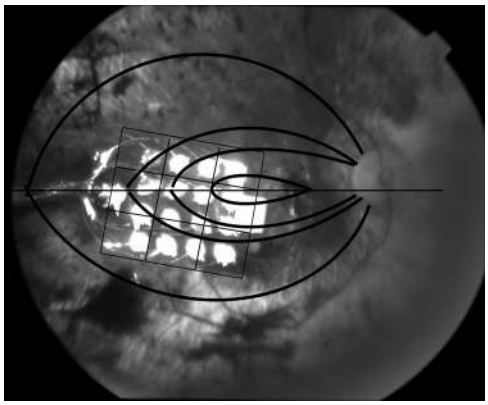

**FIGURE 2.** Fundus photo of study patient's right eye with the implanted epiretinal array. The 16-electrode epiretinal array was situated temporal to the optic disc directly over the macula. Superimposed on the photo is the 3-by-3 grid arrangement used for analysis of the retina immediately underlying the array and the coursing of the retinal nerve axons toward the optic nerve.

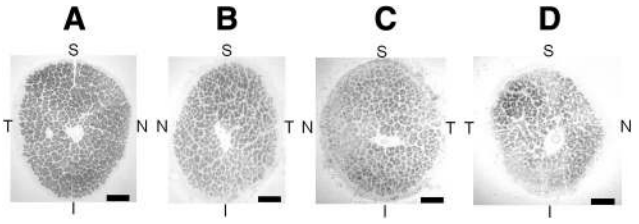


**FIGURE 3.** Paraphenylenediamine (PPD) stain of (**A**) age-matched normal optic nerve, (**B**) age-matched RP optic nerve, (**C**) patient's left optic nerve, and (**D**) patient's right optic nerve (the implant eye). PPD highlights the myelinated axons. The patient's right optic nerve demonstrates a significant amount of atrophy when compared to the left optic nerve. Atrophy is apparent by the increased connective tissue between nerve fascicles, decrease in total number of axons, and decreased overall size of the patient's right optic nerve. The temporal quadrant appears to have the greatest number of preserved axons within the right optic nerve. The patient's right and left optic nerves and RP control optic nerve appear to have significant atrophy when compared to the age-matched normal optic nerve. S, superior; T, temporal; I, inferior; N, nasal. Bar, 500 $\mu$m.

throughout the implantation period. Here, we examine the optic nerves and retina collected postmortem to characterize the changes secondary to implantation and stimulation and end-stage RP. The fellow eye is often very valuable for comparison purposes. However, severe damage to the retina in the study patient's left eye at the time of enucleation precluded such comparison. The optic nerves from both sides were compared. Furthermore, we provide comparison with retinas and optic nerves from age-matched normal patients and age-matched RP patients.

Optic nerves from the study patient and the age-matched RP patients demonstrated significant atrophy when compared with those of the age-matched normal patients, evident both histologically (Fig. 3) and morphometrically in terms of total axon counts (Fig. 4). Total axon counts using criterion 1 were 45,726 ± 3,004 in the study patient's right optic nerve;

**Total Axon Counts**

| | Criterion 1 | Criterion 2 |
|---|---|---|
| Study patient implanted, RP-affected right eye | 45,726 ± 3004 | 81,442 ± 4664 |
| Study patient non-implanted, RP affected left eye | 140,393 ± 4740 | 203,401 ± 14746 |
| Age-matched RP patient #1 | 68,096 ± 2873 | 111,311 ± 13000 |
| Age-matched RP patient #2 | 227,515 ± 1559 | 369,933 ± 21613 |
| Age-matched normal patient #1 | 750,855 ± 3983 | 993,763 ± 43741 |
| Age-matched normal patient #2 | 714,887 ± 3852 | 1,297,791 ± 42010 |

**FIGURE 4.** Total axons in each optic nerve. Optic nerves from the study patient and age-matched RP patients had fewer total axons compared to the age-matched normal patients ($P$ = 0.03 and 0.01, respectively, using criterion 1 and $P$ = 0.026 and 0.045, respectively, using criterion 2). There was no significant difference in total axons between each of the study patient's optic nerves versus the two optic nerves from RP patients ($P$ = 0.59 and 0.97 with criterion 1 and $P$ = 0.61 and 0.89 with criterion 2 for study patient's right and left optic nerves, respectively). To the *right* of the chart, *solid lines* indicate statistical significance between groups; *dashed lines* indicate lack of statistical significance.

140,393 ± 4,740 in the study patient's left optic nerve; 68,096 ± 2.873 in age-matched RP patient 1; 227,515 ± 1,559 in age-matched RP patient 2; 750,855 ± 3,983 in age-matched normal patient 1; 714,887 ± 3,852 in age-matched normal patient 2. Total axon counts using criterion 2 were 81,442 ± 4,664 in the study patient's right optic nerve; 203,401 ± 14,746 in the study patient's left optic nerve; 111,311 ± 13,000 in age-matched RP patient 1; 369,933 ± 21,613 in age-matched RP patient 2; 993,763 ± 43,741 in age-matched normal patient 1; 1,297,791 ± 42,010 in age-matched normal patient 2. Independent-samples *t*-tests of optic nerve axon counts of the study patient versus the age-matched normal patients and age-matched RP patients versus age-matched normal patients yielded $P = 0.03$ and $= 0.01$, respectively, using criterion 1 and $P = 0.03$ and $= 0.04$, respectively, using criterion 2. There was no statistically significant difference in total axon counts between each of the study patient's optic nerves versus the two optic nerves from RP patients ($P = 0.59$ and $P = 0.97$ with criterion 1, and $P = 0.61$ and $P = 0.89$ with criterion 2, for the study patient's right and left optic nerves, respectively). No statistical analysis was performed between the study patient's implanted and nonimplanted eyes, because a *t*-test cannot be performed between two groups, each having a single sample. Appropriate use of the *t*-test requires a standard deviation within the groups to be compared, and with only a single eye in each group, no standard deviation can be calculated. Therefore, the only comparison that can be made between individual eyes is strictly observational. In that regard, there did appear to be a difference between the implanted and the contralateral eye in that patient, but it is not possible in this study to determine the statistical significance of that difference. Any differences between the study patient and the age-matched RP patients were small compared with the axon dropout in age-matched normal patients versus that in age-matched RP patients.

The ratio of degenerated axon profiles to healthy axons reflected the amount of damage in each optic nerve quadrant (Figs. 5A, 5B). The study patient's right optic nerve had consistently higher ratios and therefore demonstrated more overall damage than did the fellow left optic nerve and optic nerves from the age-matched RP patients and normal patients. The study patient had a clinical history of worse VA (NLP for ~6 years before death) in the right eye. Given that there is at least a loose retinotopic order within the optic nerve immediately

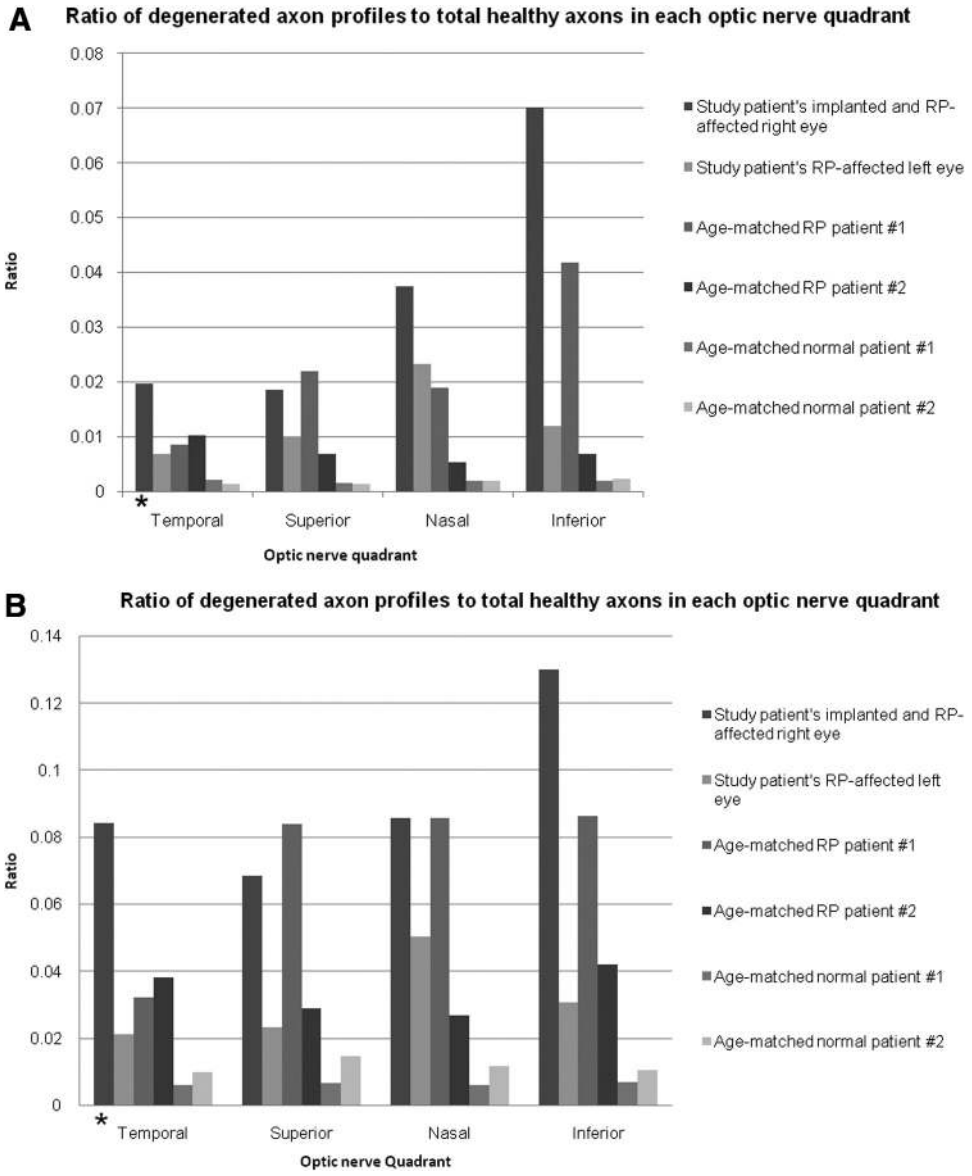


**FIGURE 5.** (**A**) Number of degenerated axon profiles relative to number of healthy axons in each optic nerve quadrant using criterion 1. Each quadrant of the implanted and RP-affected right eye showed high ratios of degenerated axon profiles to healthy axons compared to respective quadrants in the fellow left optic nerve, RP controls, and normal controls. This eye had more advanced RP disease and prior acute stimulations. However, the temporal optic nerve quadrant which corresponded to the site of epiretinal array implantation and stimulation (marked with *) had a low ratio when compared to other quadrants within the same optic nerve. The degenerated axon profiles represent an intermediate-to-late stage of an ongoing aging and/or disease process during which axons are slowly digested by macrophages and eventually removed from the nerve. (**B**) Number of degenerated axon profiles (including macrophages) relative to number of healthy axons in each optic nerve quadrant using criterion 2. Even though criterion 2 was more inclusive with both total axon and degenerated axon (and thus had slightly different absolute ratios compared to criterion 1), the two data sets still showed striking similarities in the overall pattern.

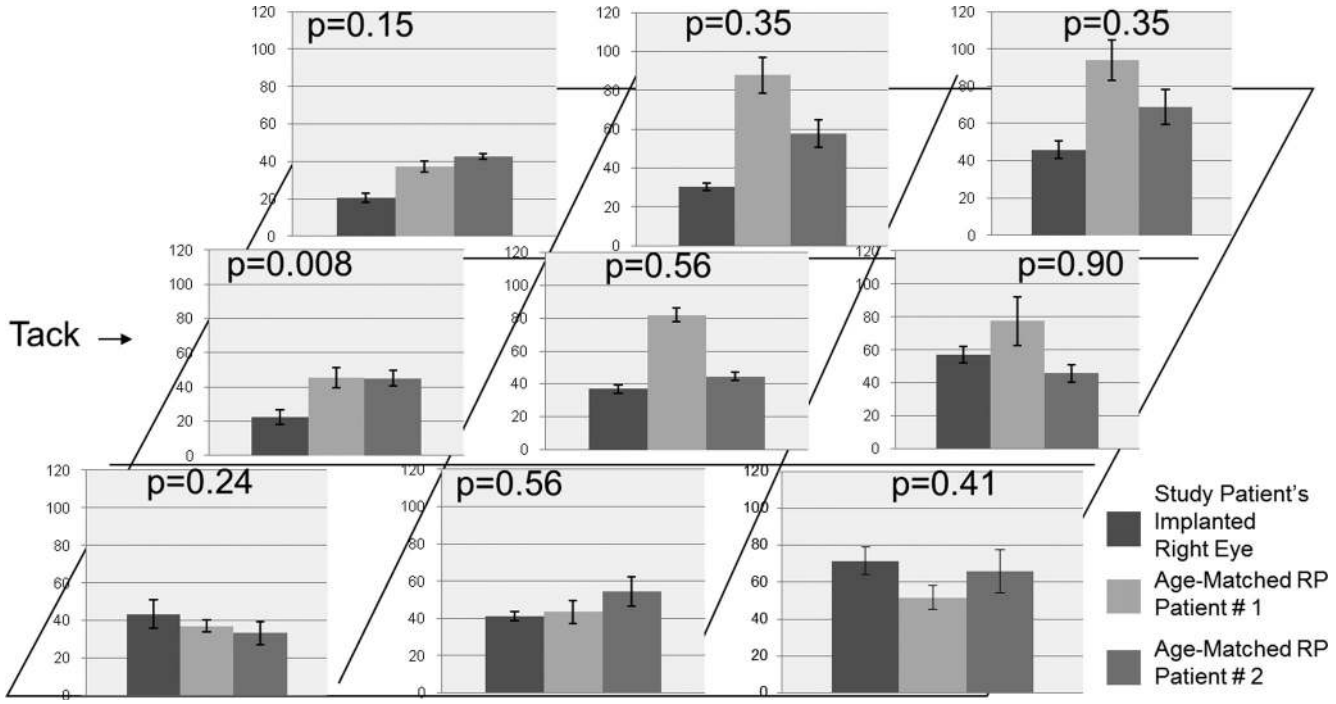


**Figure 6.** Neuron counts in retinal cross-sections taken through nine (3 × 3) regions of the perimacular area in each of the three patients. *Left column*: study patient's right eye; *middle* and *right columns*: age-matched RP patients 1 and 2, respectively. The retina underlying the prosthesis in the study patient was compared with corresponding regions of the retina in the two age-matched RP patients to give the *P* values above each graph. See Figure 2 for the locations of each region. With the exception of the tack area ($P = 0.008$), there was no significant difference in the number of neurons between the study patient and the two RP controls in the other eight regions.

posterior to the globe in humans,[15] the temporal quadrant of the study patient's right optic nerve corresponded to the perimacular region where the epiretinal array was implanted and electrical stimulation applied. This temporal quadrant did not appear to have an increased ratio in comparison with other quadrants in the study patient's right optic nerve using either criteria. The ratios in the age-matched normal patients were consistently the lowest throughout all quadrants with both criteria.

The perimacular area where the epiretinal array was situated in the study patient's right eye was compared with the same areas from the two RP patients (Fig. 6). Independent-samples *t*-tests of neuron counts in each of the nine perimacular regions of the study patient's right eye versus that in two age-matched RP patients yielded no significant differences, with the only exception being the region that included the epiretinal array tack site. The region involving the tack site in the study patient's right eye had significantly fewer neurons than did the corresponding regions in the two age-matched RP patients ($P = 0.008$). The other eight regions did not show a consistent trend that could be deemed statistically significant, especially given the small sample size. There was a fairly homogeneous expression of GFAP throughout the entire perimacular region in the study patient's right eye as well as in the two age-matched RP patients (Fig. 7). Overall, the expression of GFAP was judged to be equal among all eyes. With the exception of the region that included the tack site, none of the other eight perimacular regions located directly underneath the prosthesis in the study patient's right eye demonstrated an appreciable increase in GFAP expression. Fibrosis had completely replaced the normal retinal architecture in the immediate vicinity of the tack site. This accounted for the aforementioned decreased neuronal component in that region.

## Discussion

This study represents the first opportunity to characterize changes in the optic nerve and retina of an end-stage RP patient with long-term implantation of an epiretinal array with electrical stimulation. In the clinical trial, the study patient's right eye had been implanted and intermittently stimulated for more than 5 years. Shortly after the patient's death, the retina and optic nerve from this right eye were sectioned and morphometrically analyzed to elucidate the effects of implantation/electrical stimulation and advanced RP.

The present study found a 70% to 90% decrease in total retinal ganglion cell axon counts in RP patients compared with counts in normal patients, but could not detect a difference between our study patient and two RP patients. There have been no prior studies directly examining the optic nerve axons of end-stage RP patients, but optic atrophy was previously noted in very advanced RP.[16] The decrease in axons was also consistent with the finding of Santos et al.[17] that patients with severe RP retained an average of 30% of intact retinal ganglion cells. Quantification of ganglion cells within the retina is difficult in the normal retina, given the presence of displaced amacrine cells and other complexities. It is even more difficult in RP patients who often have disorganized retinal cell layers. Other factors contributing to particularly poor morphology of the retinal cell layers in our study patient were the long interval between death and fixation and the presence of oil in the eye. The oil invasion of the retina likely caused the extensive vacuolization, which can be appreciated along the entire length of the study patient's retina in the implanted eye. However, no stain for oil was completed to confirm this. This consideration along with the optic nerve's role in transmitting stimuli generated by the epiretinal array to the brain, led to in-depth morphometric analysis and comparison of optic nerves.

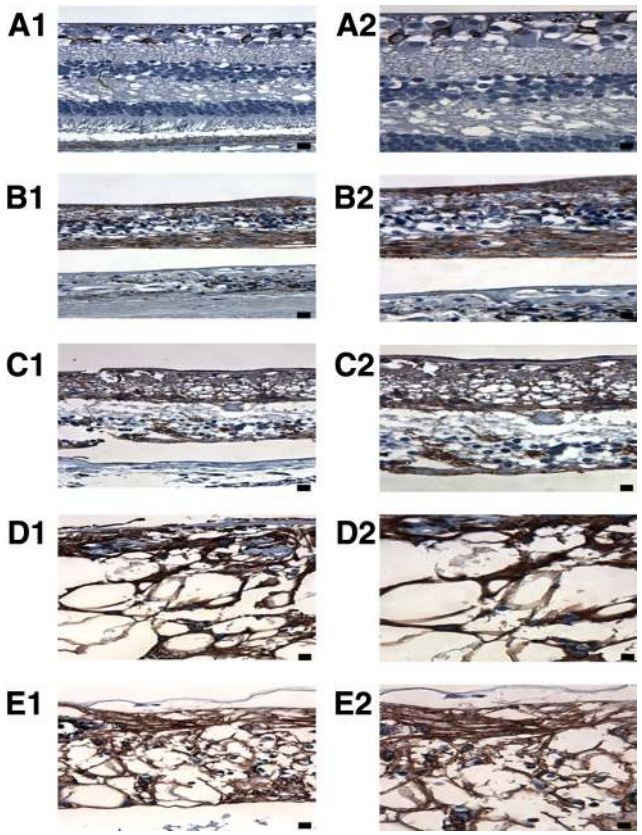


**FIGURE 7.** GFAP immunostaining of (**A**) the macula of age-matched control patient 2, (**B**) macula of age-matched RP patient 1, (**C**) macula of age-matched RP patient 2, (**D**) midperipheral retina of study patient's right eye, and (**E**) retina underlying the array in the study patient's right eye. GFAP staining in the age-matched control was localized primarily to astrocytes in the retinal ganglion cell and nerve fiber layers. RP controls and study patient retinas demonstrated fairly homogeneous GFAP expression qualitatively throughout the extent of the macular region. There were no appreciable differences in the amount of GFAP expression among the two RP controls, the midperipheral retina (**D**), and macular region (**E**) of study patient's right eye. All specimens, other than the age-matched normal control, exhibited retinoschisis (visible in **C**) and retinal detachments (visible in **B**–**E**) along their retinas. In addition, the implant patient exhibited extensive vacuolization (**D** and **E**) likely secondary to silicone oil; however, no stain was performed to prove this. *Left column* (**A1**–**E1**), 400× magnification, Bar, 25 $\mu$m. *Right column* (**A2**–**E2**), 630× magnification. Bar, 20 $\mu$m.

Several results are worth considering, notwithstanding some of the limitations intrinsic to such a study. First, total axon counts can be highly dependent on the counting technique used and the individual doing the counts. One approach is to be highly selective and count only what is definitively a healthy axon. Criterion 1 approached the counts in this manner and, as such, likely missed several smaller but more difficult to distinguish axons. Another approach is to be more inclusive, increasing the sensitivity at the expense of specificity. Criterion 2 led to the inclusion of almost all the healthy axons, but probably also some nonaxons as well. As such, the true axon counts likely fall somewhere in between the values obtained using these two criteria. Most critical to note were the internal consistency and the same statistical trends shown with each data set. Second, prior studies noted a large variation in axon counts of normal optic nerves, even when controlling for age.[18,19] There were also large differences between optic nerves from the same patient.[20] Despite the normal large variation in axon counts, the dramatic difference between the two normal and two RP patients achieved statistical significance with both criteria. Long delays to fixation (>20 hours) have been associated with lower optic nerve axon counts.[21] This may explain the difference in axon count between RP patients 1 and 2, as their eyes had time-to-fixation periods of 39 hours versus 12 hours, respectively. Likewise, the 70-hour time to fixation for the study patient may have resulted in artificially depressed axon counts. Finally, it is important to note that many of the remaining ganglion cells and their axons coursing through the optic nerve from the macula were functional, as indicated by the patient's ability to detect electrically elicited phosphenes. This was in spite of a decreased axon count that was most likely secondary to an ongoing process of transneuronal degeneration. It had been suggested in previous studies that electrical stimulation has a neuroprotective effect in promoting retinal ganglion cell axon health[22] and even in rescuing axotomized retinal ganglion cells.[23,24]

Despite having significantly fewer total optic nerve axons in the RP patients and the study patient, the number of degenerated axon profiles was not proportionately increased in these optic nerves. Degenerated axon profiles are formed when five to eight degenerated axons are aggregated by macrophages and then surrounded by a new myelin ring.[25] Criterion 1 did not include degenerated axons inside macrophages, but criterion 2 did. The ratio of degenerated to healthy axons accounted for the different stages of degeneration in the optic nerve by factoring in the number of remaining healthy axons. On this basis, we saw that the study patient's right optic nerve had more damage than the other nerves, but that there was not an appreciable increase in damage in the temporal quadrant of the study patient's right optic nerve relative to the other quadrants within the same nerve. The same trends were shown with both criteria.

Optic nerve changes secondary to epiretinal array implantation and stimulation may have been preceded by retinal changes in a process similar to transneuronal degeneration.[16,26] However, morphometric analysis of the perimacular retina (implanted region) in the study patient versus the perimacular retinas in two age-matched RP patients disclosed no evidence of damage within the retina underlying the array, except for the tack site. The tack used for fixation of the prosthesis to the retina was designed to penetrate all layers of the retina and through the sclera. Therefore, it was not surprising to find significant fibrosis replacing neurons in the area immediately surrounding the tack insertion site. Previous studies described similar changes around tacks used to attach prostheses to the retina, including retinal pigment epithelium hyperpigmentation[6] or scarring, epiretinal membrane formation, and retinal folds.[8] GFAP stained intensely throughout the retina of all three eyes, consistent with the cellular hypertrophy and reactive gliosis of Müller cells and reactive hyperplasia of astrocytes in RP retinas.[27] In our study patient, the lack of increased GFAP expression in the retina underneath the array (with the exception of the tack site) suggested that there was no major injury due to pressure applied by the array against the retina. This conclusion was also consistent with the assessment of the neuronal component within the retina, using NSE.

The comparison of the study patient against two age-matched RP patients was effective in isolating retinal changes secondary to epiretinal array implantation and stimulation, despite the inherent limitations. One such limitation was that, because of the difficulty in obtaining quality specimens from 80-year-old RP patients without significant ocular co-morbidities, the inheritance pattern of RP in our control patients was different from that in our study patient. However, the severity of RP as determined by visual acuity had been found to be more closely associated with significant differences in outer nuclear layer counts and ganglion cell layer counts than the

inheritance pattern.[17] Another limitation included the disorganized retinal cell layers that prevented more detailed morphometric analysis of the retina such as retinal cell layer counts and retinal thickness. The small sample size also limited the conclusions that could be generated.

The patient in the current pilot investigation had undergone successful implantation, followed by stimulation for more than 5 years and thus, provides a valuable basis for morphometric and histologic comparison. This pilot study also distinguished some of the effects of end-stage RP that must be separated from the effects due to implantation and stimulation. Future studies will further elucidate the effects of long-term epiretinal array implantation and electrical stimulation.

## *Acknowledgments*

The authors thank The Foundation Fighting Blindness for providing the RP specimens.

## *References*

1. Humayun MS, de Juan E Jr., Dagnelie G, et al. Visual perception elicited by electrical stimulation of retina in blind humans. *Arch Ophthalmol.* 1996;114(1):40–46.
2. Margalit E, Maia M, Weiland JD, et al. Retinal prosthesis for the blind. *Surv Ophthalmol.* 2002;47(4):335–356.
3. Sachs HG, Gabel VP. Retinal replacement–the development of microelectronic retinal prostheses–experience with subretinal implants and new aspects. *Graefes Arch Clin Exp Ophthalmol.* 2004; 242(8):717–723.
4. Hesse L, Schanze T, Wilms M, et al. Implantation of retina stimulation electrodes and recording of electrical stimulation responses in the visual cortex of the cat. *Graefes Arch Clin Exp Ophthalmol.* 2000;238(10):840–845.
5. Jensen RJ, Ziv OR, Rizzo JF 3rd. Thresholds for activation of rabbit retinal ganglion cells with relatively large, extracellular microelectrodes. *Invest Ophthalmol Vis Sci.* 2005;46(4):1486–1496.
6. Majji AB, Humayun MS, Weiland JD, et al. Long-term histological and electrophysiological results of an inactive epiretinal electrode array implantation in dogs. *Invest Ophthalmol Vis Sci.* 1999;40(9): 2073–2081.
7. Rizzo JF 3rd, Wyatt J, Loewenstein J, et al. Methods and perceptual thresholds for short-term electrical stimulation of human retina with microelectrode arrays. *Invest Ophthalmol Vis Sci.* 2003; 44(12):5355–5361.
8. Walter P, Szurman P, Vobig M, et al. Successful long-term implantation of electrically inactive epiretinal microelectrode arrays in rabbits. *Retina.* 1999;19(6):546–552.
9. Humayun MS, Weiland JD, Fujii GY, et al. Visual perception in a blind subject with a chronic microelectronic retinal prosthesis. *Vision Res.* 2003;43(24):2573–2581.
10. Weiland JD, Humayun MS, Dagnelie G, et al. Understanding the origin of visual percepts elicited by electrical stimulation of the human retina. *Graefes Arch Clin Exp Ophthalmol.* 1999;237(12): 1007–1013.
11. Yanai D, Weiland JD, Mahadevappa M, et al. Visual performance using a retinal prosthesis in three subjects with retinitis pigmentosa. *Am J Ophthalmol.* 2007;143(5):820–827.
12. Humayun MS, de Juan E Jr., Weiland JD, et al. Pattern electrical stimulation of the human retina. *Vision Res.* 1999;39(15):2569–2576.
13. Chan SO, Guillery RW. Changes in fiber order in the optic nerve and tract of rat embryos. *J Comp Neurol.* 1994;344(1):20–32.
14. Sadun AA, Smith LE, Kenyon KR. Paraphenylenediamine: a new method for tracing human visual pathways. *J Neuropathol Exp Neurol.* 1983;42(2):200–206.
15. Fitzgibbon T, Taylor SF. Retinotopy of the human retinal nerve fibre layer and optic nerve head. *J Comp Neurol.* 1996;375(2): 238–251.
16. Gartner S, Henkind P. Pathology of retinitis pigmentosa. *Ophthalmology.* 1982;89(12):1425–1432.
17. Santos A, Humayun MS, de Juan E Jr., et al. Preservation of the inner retina in retinitis pigmentosa. A morphometric analysis. *Arch Ophthalmol.* 1997;115(4):511–515.
18. Mikelberg FS, Yidegiligne HM, Schulzer M. Optic nerve axon count and axon diameter in patients with ocular hypertension and normal visual fields. *Ophthalmology.* 1995;102(2):342–348.
19. Repka MX, Quigley HA. The effect of age on normal human optic nerve fiber number and diameter. *Ophthalmology.* 1989;96(1): 26–32.
20. Johnson BM, Miao M, Sadun AA. Age-related decline of human optic nerve axon populations. *Age.* 1987;10:5–9.
21. Balazsi AG, Rootman J, Drance SM, et al. The effect of age on the nerve fiber population of the human optic nerve. *Am J Ophthalmol.* 1984;97(6):760–766.
22. Goldberg JL, Espinosa JS, Xu Y, et al. Retinal ganglion cells do not extend axons by default: promotion by neurotrophic signaling and electrical activity. *Neuron.* 2002;33(5):689–702.
23. Watanabe M, Fukuda Y. Survival and axonal regeneration of retinal ganglion cells in adult cats. *Prog Retin Eye Res.* 2002;21(6):529–553.
24. Morimoto T, Miyoshi T, Matsuda S, et al. Transcorneal electrical stimulation rescues axotomized retinal ganglion cells by activating endogenous retinal IGF-1 system. *Invest Ophthalmol Vis Sci.* 2005; 46(6):2147–2155.
25. Johnson BM, Sadun AA. Ultrastructural and paraphenylene studies of degeneration in the primate visual system: degenerative remnants persist for much longer than expected. *J Electron Microsc Tech.* 1988;8(2):179–183.
26. Stone JL, Barlow WE, Humayun MS, et al. Morphometric analysis of macular photoreceptors and ganglion cells in retinas with retinitis pigmentosa. *Arch Ophthalmol.* 1992;110(11):1634–1639.
27. Milam AH, Li ZY, Fariss RN. Histopathology of the human retina in retinitis pigmentosa. *Prog Retin Eye Res.* 1998;17(2):175–205.